Contr. Mineral. and Petrol. 25, 77—94 (1970)

Functions Describing Preferred Orientation in Flat Aggregates of Flake-Like Clay Minerals and in Other Axially Symmetric Fabrics*

FRIEDRICH LIPPMANN
Mineralogisches Institut der Universität Tübingen

Received June 4, 1969

Abstract. The oriented aggregates of flake-like clay minerals, prepared in the laboratory for X-ray identification purposes, are axially symmetric fabrics, with the axis of symmetry or pole perpendicular the surface. The density of the vectors normal to the basal planes of the clay particles has its maximum at the pole. A given number of particles is considered, and the degree of orientation is assumed variable with one single parameter t, defined as maximum density over constant average density $\bar{D}$. The decline of the basal vector density from the pole to the equator may then be described by a power of the cosine of the polar angle φ:

$$D(\varphi, t) = t \cdot \bar{D} \cdot (\cos \varphi)^{t-1}. \quad (9)$$

This formula yields a quantitative description of orientation patterns measured on artificial fabrics by means of X-ray diffraction and on the universal stage.

In some cases, the description may be refined by using a function composed of two additive cosine powers. The cosine power is by no means a mathematically unique solution but other possible functions are less versatile and yield no better fit with the experimental data. The Gauss distribution may be regarded as an approximation of (9) for very high degrees of orientation.

Introduction

Oriented aggregates of flake-like clay particles are commonly prepared in the laboratory in order to obtain enhanced basal reflections in X-ray diffraction for identification purposes. An enhancement also of the diagnostically important $(0k0)$ reflections may be achieved in a suitably aligned Guinier camera by the use of oriented aggregates as well (Lippmann, 1968). These preparations, flake-like themselves, albeit on a much larger scale than the individual particles, must be expected to exhibit axial symmetry with the axis of symmetry perpendicular to the flake surface. The various techniques of preparing oriented clay aggregates do not deliberately aim at axial symmetry. It is more a by-product of the efforts to obtain a homogeneous clay film with a constant thickness over the whole face. To this end, nothing is done which might create a privileged direction within the plane of the specimen. Such a direction, if present, would have to be described by an azimuth angle, i.e. by an angle with some reference direction in the specimen surface, e.g. with a slide edge. From the absence of any process which might bring about an azimuthal dependence of orientation during specimen preparation we may conclude that the resulting oriented aggregates are indeed axially symmetric.

* Herrn Prof. Dr. Wolf v. Engelhardt zum 60. Geburtstag gewidmet.

Thus, in order to produce oriented aggregates with as high a degree of reproducibility as possible the *a priori* conditions for axial symmetry are carefully observed in most clay laboratories. The most important condition is the exactly horizontal positioning of the slides during sedimentation of the clay minerals from suspension. When the direction perpendicular to the slide coincides with the direction of gravity there exists obviously no cause for an azimuthal dependence of orientation. Although at first sight horizontal positioning does not appear important in the method of suction through a porous plate because the mean direction of suction is by all means perpendicular to the surface it is nevertheless to be maintained as far as possible in order to arrive at a constant thickness of the clay film over the whole plate.

In the method of producing preferred orientation by compression, axial symmetry is secured by the parallel alignment of piston surface and support as well as by the direction of pressure perpendicular to both.

Some investigators (e.g. Jasmund, 1950) attribute an important rôle to dry-shrinkage in bringing about preferred orientation, in the techniques using wet clays. Only if supports of excessively elongate proportions are used deviations from axial symmetry may be expected. There is, however, one type of clay aggregates, the smear mounts, in which a privileged azimuthal direction ensues from the mode of preparation. They are perhaps the only type of artificial clay aggregates for which axial symmetry does not apply, although much of their azimuthal asymmetry may be expected to disappear by shrinkage on drying.

The following considerations apply also to orientation patterns encountered in petrofabric analysis as far as they are axially symmetric. Although patterns belonging exactly to this type seem to be extremely rare, judging from the many petrofabric diagrams published by Sander (1950), axially symmetric patterns should be of considerable interest in petrofabric studies because they constitute the simplest type of preferred orientation as they are characterized by a sole privileged direction. Moreover, many petrofabric patterns of more complicated symmetry are conveniently described as axially symmetric for a first approximation.

Development of Density Function for Axially Symmetric Fabrics

In a flat oriented aggregate the vectors normal to invidual clay mineral flakes cluster around the normal to the layer. An analogous situation is encountered in many axially symmetric (or nearly so) petrofabric patterns when the directions of a suitably chosen crystallographic vector are concentrated around the axis of symmetry. The maximum density of such vectors may then be used to describe the degree of preferred orientation.

In order to quantify our considerations we follow Taylor and Norrish (1966) and assign one vector to each particle in a fabric of uniform grain size. For non-uniform grain size distributions, the number of vectors assigned to any one particle may be thought proportional to its volume. The density of the vectors in a given spot of the unit sphere may then be defined as the number of vectors per unit solid angle, i.e. per unit area on the surface of the unit sphere. The position of a certain

vector is described in spherical polar coordinates by the polar angle φ, which denotes the angular distance from the axis of symmetry or pole, and by the azimuth angle ψ, which defines the position of the projection of a vector on the equator. This latter coincides with the specimen surface in oriented clay aggregates, and it is generally defined as the great circle perpendicular to the pole.

For a certain crystallographic vector, a given orientation pattern of any symmetry may be described by the density of the vector as a function of the spherical coordinates ψ and φ. If this function $D(\psi, \varphi)$ is known it is possible to calculate the average vector density $\bar{D}$ on the unit hemisphere (area 2π):

$$\bar{D} = \frac{\int_0^{2\pi} \int_0^{\pi/2} D(\psi, \varphi) \cdot \sin \varphi \, d\varphi \, d\psi}{2\pi}. \tag{1}$$

For a given material this average density is independent of the special type of orientation pattern provided that a constant specimen volume is considered. This condition is automatically satisfied in X-ray diffraction when operating with a given slit system and when all of the primary beam is absorbed by the specimen (Klug and Alexander, 1954). $\bar{D}$ then also determines the diffracted intensity from a specimen with completely random orientation or uniform spatial distribution of the crystallographic vectors. In microscopic petrofabric work, $\bar{D}$ is either equivalent to the number of grains measured and scaled to equal grain size, or to the area of thin section studied.

For axially symmetric fabrics, $D(\psi, \varphi) = D(\varphi)$ is independent of ψ and is a function only of the polar distance φ. (1) therefore simplifies to:

$$\bar{D} = \int_0^{\pi/2} D(\varphi) \cdot \sin \varphi \, d\varphi. \tag{2}$$

At this moment, all we know about $D(\varphi)$ is that it assumes its maximum value $D_{\max}(\varphi)$ exactly on the axis of symmetry:

$$D_{\max}(\varphi) = D(\varphi = 0).$$

For fabrics consisting of identical material and studied under the same experimental conditions, the magnitude of $D(\varphi = 0)$ ($D(0)$ in the following) may be used as a measure for preferred orientation. An orientation index t which is independent of experimental set-up is obtained by referring $D(0)$ to $\bar{D}$:

$$\text{for clays:} \quad t_{(0\,0\,l)} = \frac{D(0)}{\bar{D}}; \qquad \text{in general:} \quad t = \frac{D(0)}{\bar{D}}.$$

For X-ray diffractometer measurements this procedure is equivalent to referring the basal intensity of an oriented aggregate of clay minerals to the basal intensity of a preparation with random orientation. In petrofabric studies the maximum density is referred to the total number of grains measured per unit solid angle.

For varying degree of orientation the density distribution of axially symmetric patterns may now be expressed as a function of the polar angle φ and of t, the

orientation index: $D(\varphi, t)$. Since for $\varphi = 0$ we have $D(0, t) = t \cdot \bar{D}$ one may assume that the factors t and $\bar{D}$ are contained in $D(\varphi, t)$ also for $\varphi \neq 0$, hence:

$$D(\varphi, t) = t \cdot \bar{D} \cdot E(\varphi, t) \tag{3}$$

$E(\varphi, t)$, like $D(\varphi, t)$, assumes its maximum value for $\varphi = 0$, but this maximum is identical to 1 regardless of t:

$$E(0, t) \equiv 1.$$

Nevertheless, $E(\varphi, t)$ has to be a function also of t, to render possible a variable decrease of the density with increasing φ for varying degrees of orientation. By substituting (3) in (2) we have:

$$\bar{D} = \int_0^{\pi/2} t \cdot \bar{D} \cdot E(\varphi, t) \cdot \sin\varphi \, d\varphi.$$

Since t and $\bar{D}$ are independent of φ:

$$1 = t \cdot \int_0^{\pi/2} E(\varphi, t) \cdot \sin\varphi \, d\varphi; \qquad \frac{1}{t} = \int_0^{\pi/2} E(\varphi, t) \cdot \sin\varphi \, d\varphi. \tag{4}$$

The function $E(\varphi, t)$ has now to be determined is such a way as to satisfy the preceding relation (4). The substitution

$$\frac{d\cos\varphi}{d\varphi} = -\sin\varphi; \qquad \frac{1}{t} = \int_{\pi/2}^{0} E(\varphi, t) \, d\cos\varphi \tag{5}$$

suggests that $E(\varphi, t)$ may be replaced by a function of $\cos\varphi$:

$$E(\varphi, t) = F(\cos\varphi, t); \qquad \frac{1}{t} = \int_{\pi/2}^{0} F(\cos\varphi, t) \, d\cos\varphi, \tag{6}$$

$$\cos\varphi = z; \qquad \frac{1}{t} = \int_0^1 F(z, t) \, dz. \tag{7}$$

The desired value of $1/t$ for the integral results for:

$$F(z, t) = z^{t-1}. \tag{8}$$

Taking account of (8) and reversing substitutions (7) and (6) we obtain:

$$E(\varphi, t) = F(\cos\varphi, t) = (\cos\varphi)^{t-1}.$$

By substituting this in (3), the density function for axially symmetric fabrics is expressed by:

$$D(\varphi, t) = t \cdot \bar{D} \cdot (\cos\varphi)^{t-1} \tag{9}$$

or:

$$D(\varphi, t) = D(0) \cdot (\cos\varphi)^{t-1}. \tag{9a}$$

So far our considerations have been limited to the upper hemisphere where $\cos\varphi$ is positive. Since only positive real values of a density are meaningful in practice

but since on the lower hemisphere $(\cos\varphi)^{t-1}$ may assume negative or imaginary values for variable $(t-1)$ we may write for the moment:

$$D(\varphi, t) = t \cdot \bar{D} \cdot (\cos^2 \varphi)^{\frac{t-1}{2}} \tag{9b}$$

or:

$$D(\varphi, t) = t \cdot \bar{D} \cdot |\cos \varphi|^{t-1} \tag{9c}$$

if we want to apply the density function also for the lower hemisphere. This procedure is justified as long as the crystallographic vectors, of which we study the distribution, are non-polar. Even if polar vectors do occur almost all of the current experimental methods for determining vector densities are not sensitive to polarity. Therefore, in general, the distribution on the lower hemisphere will be the mirror image of that on the upper one, and exactly this is conveyed by writing (9b) or (9c) instead of (9).

When plotting $D(\varphi, t)$ versus φ according to (9) or (9a—c) we trace bell-shaped curves which have their maxima at $\varphi = 0$. They are different from Gauss curves, which are zero only at $\pm\infty$, in that the zeros of $(\cos\varphi)^{t-1}$ are at $\pm\frac{\pi}{2}$; with one possible exception: for $t = 1$, which characterizes random orientation, the zero at $\frac{\pi}{2}$ may be smoothed out by an infinitesimal process. With increasing t the maxima of the bell-shaped curves become more and more pronounced, and the function approaches almost zero at lower and lower values of φ. Before entering into a further discussion of the function, which up to now is of purely theoretical significance, it is important to show to what extent it is capable of portraying experimental data.

Application of Developed Function to Experimental Data

Continuing the experiments of v. Engelhardt and Gaida (1963) on the compaction of clay minerals, Thiem (1967) undertook a quantitative X-ray measurement of the orientation of samples of kaolinite and montmorillonite. These clay minerals had been subjected to various pressures in the piston-cylinder apparatus, which had been used before by the former authors. The X-ray measurements were carried out on a diffractometer of about the same type as that introduced by Schulz (1949). The most important additional feature by which the diffractometer is distinguished from ordinary X-ray diffractometers is a tilting mechanism which allows to incline the specimen, in the direction perpendicular to the plane of the focusing circle, from its regular position ($\varphi = 0°$) by various φ-angles. Since the slits confining the primary beam were of such dimensions that it is absorbed entirely by the specimen up to the maximum φ-angles of $\pm 75°$ the basal intensities measured as a function of φ, $J(\varphi, t)$, are proportional to the vector density $D(\varphi, t)$. The same relations as have been defined and developed above for D may thus be written for J as well. E.g., the average intensity $\bar{J}$, i.e. the intensity of a randomly oriented specimen, is related to the intensity function $J(\varphi, t)$ by the analogue of (2):

$$\bar{J} = \int_0^{\pi/2} J(\varphi, t) \cdot \sin\varphi \, d\varphi \quad \text{(conf. Jetter } et\ al.\text{, 1956).}$$

Therefore, Thiem multiplied his measured $J(\varphi)$ values by $\sin \varphi$, plotted the resulting values versus φ, and determined $\bar{J}$ by graphical integration. The degree of orientation is then:

$$t = \frac{J(0)}{\bar{J}}.$$

If indeed the above developed expression is valid then there are more convenient ways of determining $\bar{J}$ and t. The following procedure yields, at the same time, the possiblity of checking the validity of the analogue of (9):

$$J(\varphi, t) = t \cdot \bar{J} \cdot (\cos \varphi)^{t-1}. \tag{9d}$$

Instead, we may write:

$$\log J(\varphi, t) = \log (t \cdot \bar{J}) + (t-1) \cdot \log \cos \varphi. \tag{9e}$$

If we plot the logarithms of the experimental $J(\varphi)$ values versus $\log \cos \varphi$ a straight line should result. This is shown for the data of Thiem in Figs. 1 and 2. The measured points lie indeed on straight lines within the limits of experimental accuracy for the montmorillonite and also for the kaolinite. Only for the more perfectly oriented specimens of the latter, the measured intensities appear to be somewhat high at higher φ-angles. These deviations occur, however, at intensities which are so low that their significance might be questioned. We shall, nevertheless, give some more thought to these deviations later on.

The straight lines, drawn through the experimental points of the logarithmic plots, have $(t-1)$ as their slopes according to (9e). This determination of t, which involves the measurement of the angles of the straight lines with the horizontal by means of a protractor, obviates the plotting of $J(\varphi) \cdot \sin \varphi$ and the cumbersome graphical integration to obtain $\bar{J}$.

The plot of the function $J(\varphi) \cdot \sin \varphi$ (not illustrated in this paper) offers, however, an interesting way for an independent determination of t. The function is zero for $\varphi = 0°$, raises to a maximum with increasing φ, and gradually decreases towards zero as φ approaches 90°. The angle $\varphi_{\max}$ of the position of the maximum decreases with increasing perfection of orientation. This behavior of Thiem's plots suggested to search for a quantitative relationship. According to (9) we may write:

$$y = D(\varphi, t) \cdot \sin \varphi = t \cdot \bar{D} \cdot (\cos \varphi)^{t-1} \cdot \sin \varphi.$$

To find the maximum, we differentiate with respect to φ:

$$\frac{dy}{d\varphi} = t \cdot \bar{D} \cdot \left(-\sin \varphi \cdot (t-1) \cdot (\cos \varphi)^{t-2} \cdot \sin \varphi + (\cos \varphi)^{t-1} \cdot \cos \varphi\right)$$

$$\frac{dy}{d\varphi} = t \cdot \bar{D} \cdot (\cos \varphi)^{t-2} \left(\cos^2 \varphi - (t-1) \cdot \sin^2 \varphi\right).$$

For the maximum the derivative $dy/d\varphi$ has to be zero. Apart from the trivial zero at 90°, caused by the cosine factor and corresponding to a minimum, $dy/d\varphi$ will vanish when the term in parentheses is zero. The anticipated relationship is then:

$$\cot \varphi_{\max} = \sqrt{t-1}. \tag{10}$$

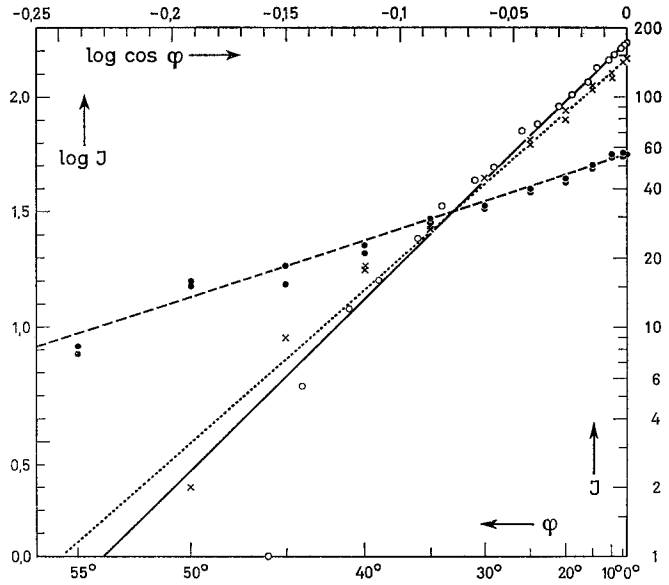

Fig. 1. Logarithmic plot according to (9e) of experimental intensities of (*001*)-reflection for specimens of montmorillonite from Cyprus; fraction $< 2\,\mu$ ⌀, with varying degree of orientation: ○○○ M II; ××× M III; ●●● M I

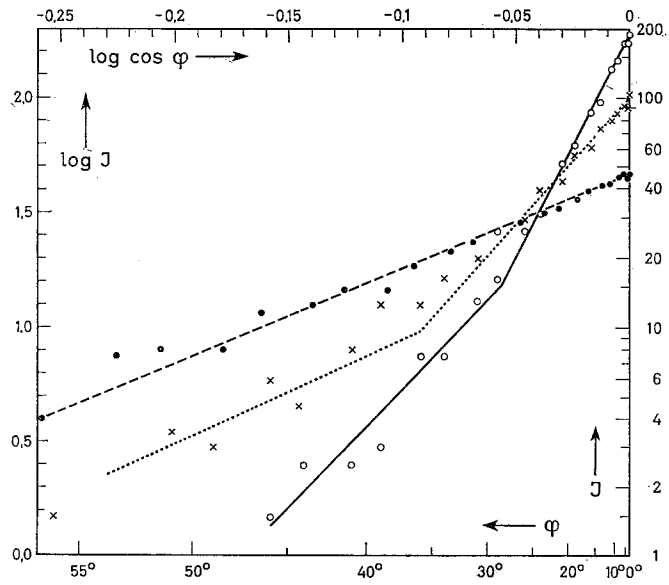

Fig. 2. Logarithmic plot according to (9e) of experimental intensities of (*002*)-reflection for specimens of kaolinite "Suprême"; fraction $< 2\,\mu$ ⌀, with varying degree of orientation: ○○○ K 6_2; ××× K 16_4; ●●● K I.

The slopes decrease with increasing φ for K 6_2 and K 16_4. Therefore, two different slopes are drawn. They correspond to the two t-coefficients used in description by two cosine powers according to (14)

Table 1. *t-values determined by different methods of evaluation*

Specimen	Preparation	Slope of logarithmic plot (9e)	Plot of $J(\varphi)\cdot\sin\varphi$ (Thiem)	
			position of maximum (10)	by graphical integration
Montmorillonite, Cyprus, air-dry; $<2\,\mu\,\varnothing$; *(001)*-reflection				
M II	collected from suspension on membrane filter	10.7	10.5—11.7	11.3
M III	compression of wet paste 132 kp/cm²	9.7	10.5—9.7	9.8
M I	compression of dry powder 200 kp/cm²	4.25	4.25	3.7
Kaolinite "Suprême"; $<2\,\mu\,\varnothing$; *(002)*-reflection				
$K\,6_2$	compression of wet paste 500 kp/cm²	21.0	19.5—22.8	20.2
$K\,16_4$	compression of wet paste 2000 kp/cm²	11.8	13.0—11.7	10.7
K I	compression of dry powder 60 kp/cm²	5.1	5.0—4.8	5.0

The t values determined by the different methods, as well as the sample descriptions, are summarized in Table 1. The agreement is of the same order of magnitude as the accuracy, of about $\pm 5\%$, with which intensities can be read from the recording of an X-ray diffractometer when no special precautions are used. The precision of the t values derived from (10) is poorest because the measurements were not planned for this purpose. The maxima were rather poorly defined on account of the spacing of 5° φ of the measurements. Better results may be expected from more closely spaced measurements in the critical region of the maximum in the $J(\varphi)\cdot\sin\varphi$ plot.

The t values derived from the logarithmic plots were used to trace intensity curves according to (9) for a more direct comparison with the experimental data than has been possible in the logarithmic diagrams. Figs. 3 and 4 show that functions of the type (9) afford a realistic description of the preferred orientation of the flake-like clay minerals.

An additional test of the validity of (9) is provided by the values of $\bar{J}$ calculated from the orientation data. They should be constant for a given mineral regardless of the degree of orientation. This is confirmed, within limits, by the $\bar{J}$ values listed in Table 2. In the case of the montmorillonite the parallelism of the $\bar{J}$ obtained from the logarithmic plot and those from integration is particularly striking, although the deviation of M I from M II and M III is considerable. M I was prepared by dry compression, in contrast to M II and M III, which were prepared in the presence of water. Most probably the deviation is due to the variability of the basal intensity of the expandable clay mineral with moisture content, i.e. M I is not strictly the same material as M II and M III.

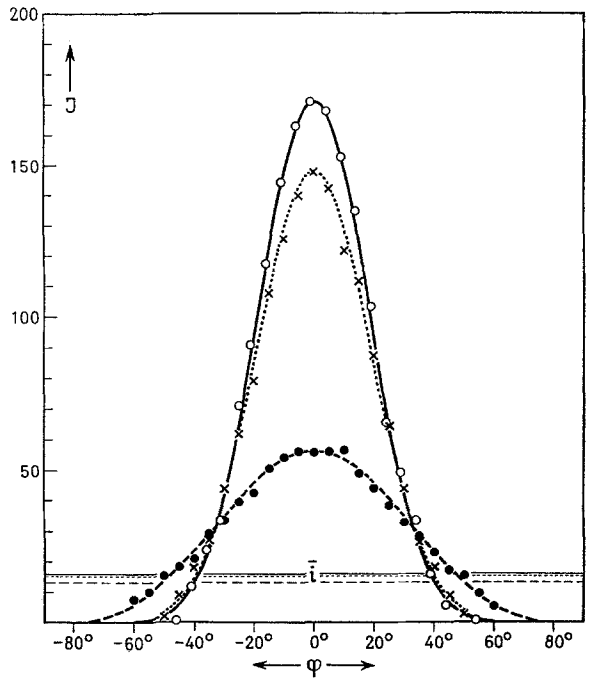

Fig. 3. Comparison of experimental (*001*)-intensities for montmorillonite from Cyprus; fraction $< 2\,\mu$ ⌀, ○○○ M II; × × × M III; ●●● M I; with calculated functions of type (9):

$$J(\varphi) = t \cdot \bar{J} \cdot (\cos\varphi)^{t-1},$$

M II: $J(\varphi) = 10.7 \cdot 16.0 \cdot (\cos\varphi)^{9.7}$; ——

M III: $J(\varphi) = 9.7 \cdot 15.2 \cdot (\cos\varphi)^{8.7}$; ·····,

M I: $J(\varphi) = 4.25 \cdot 13.2 \cdot (\cos\varphi)^{3.25}$; - - - - - -.

The intensities $\bar{J}$ according to (9), which the specimens would yield from a randomly oriented fabric, are shown as horizontal lines with corresponding signatures

For the kaolinite the agreement among the $\bar{J}$ values for one particular method is remarkable. The low values from the logarithmic plots reflect the somewhat incomplete duplication of the intensities at higher φ-angles by a function of type (9). The deviations are, nevertheless, within the limits of accuracy X-ray intensity determinations.

It appeared desirable to try function (9) also on microscopically determined petrofabric patterns. The only data, thus far found in the literature, which are readily amenable to such an evaluation, are those of Green II (1967). The pattern is that of a quartz fabric which was artificially produced by annealing a flint cylinder at 900° C and 6 kilobars (sample DT 460). The pattern of the c-axes of the quartz grains, which was determined by universal stage measurements, is axially symmetric within the limits of experimental accuracy, and the numerical density values can be read from Green's histogram. Their logarithms are plotted against log cos φ in Fig. 5. The resulting points form a straight line with fair approximation. That the points of lowest densities fall off the straight line, is due to the small

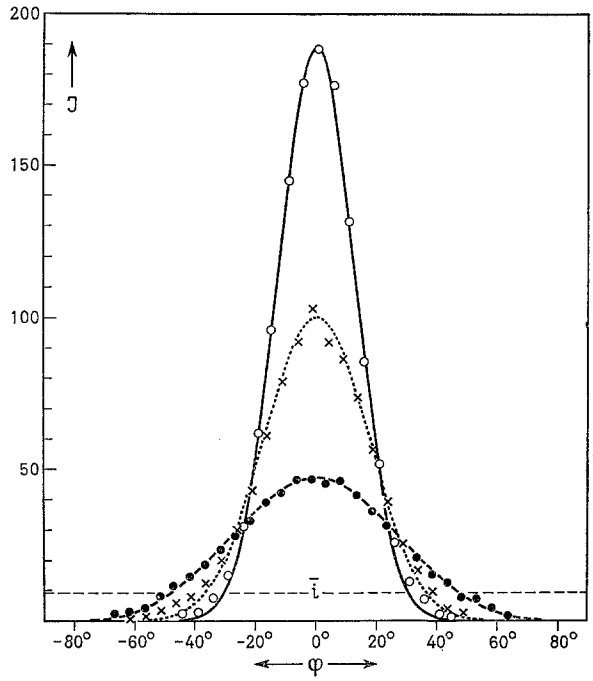

Fig. 4. Comparison of experimental (*002*)-intensities of kaolinite "Suprême"; fraction $< 2\ \mu\ \varnothing$, ○○○ K 6_2; ××× K 16_4; ●●● K I;
with calculated functions of type (9):

$$J(\varphi) = t \cdot \bar{J} \cdot (\cos\varphi)^{t-1},$$

K 6_2: $J(\varphi) = 21.0 \cdot 8.96 \cdot (\cos\varphi)^{20.0}$; ——,

K 16_4: $J(\varphi) = 11.8 \cdot 8.44 \cdot (\cos\varphi)^{10.8}$; ·····,

K I: $J(\varphi) = 5.1 \cdot 9.16 \cdot (\cos\varphi)^{4.1}$; ------.

The average intensity $\bar{J}$ is marked by the dashed horizontal line

Table 2. *Average intensities $\bar{J}$ from different methods*

Specimen	Slope of logarithmic plot (9e)	Graphical integration of $J(\varphi) \cdot \sin\varphi$ (Thiem)
M II	16.0	16.1
M III	15.2	15.6
M I	13.2	13.8
mean	14.8	15.2
K 6_2	8.96 (9.16)[a]	9.63
K 16_4	8.44 (9.16)[a]	9.22
K I	9.16	9.14
mean	8.85 (9.16)[a]	9.33

[a] Value used in description by two cosine powers (14) (Fig. 6).

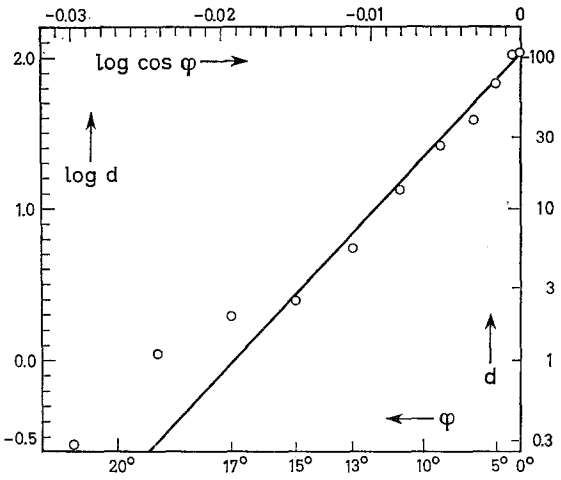

Fig. 5. Logarithmic plot of universal stage measurements by Green II on artificial quartz fabric (sample DT 460), showing extreme preferred orientation;

$$\text{ordinate} = \text{reduced density} = d = \frac{D(\varphi)}{\bar{D}},$$

$$200 \text{ grains measured:} \quad \bar{D} = \frac{200}{2\pi} = 31{,}8$$

number of grains (4; 2 and 1, respectively) which they represent among the 200 grains measured in total. According to the slope of the straight line t is 105, which is almost identical with 107, the value determined directly by Green as the reduced maximum density in the pole figure.

Discussion

It may seem surprising that it has been possible to develop a function describing the angular dependence of vector density, without recourse to concrete models concerning the mechanism which might bring about preferred orientation. We are, however, in a similar situation when we develop the vapor pressure formula

$$\ln p = \frac{-H}{RT} + C$$

from thermodynamic principles.

In doing so, we rely on the first and second laws of thermodynamics, i.e. on *conservation principles*, and on the law of the ideal gas, the simplest equation of state available for the vapor phase. We need not consider the detailed mechanisms by which the molecules are held back in the condensed phase. The acting forces, which may be of very different character, are summarized by just one parameter, the heat of evaporation H. Nevertheless, the resulting formula has proved, in countless experiments, that it adequately, or at least approximately, describes the temperature dependence of the vapor pressure of both liquids and solids, held together by all possible types of bonding forces. Therefore, it is now in constant use for the interpolation as well as extrapolation of experimental data.

The postulates used for developing our function (9) are in many respects analogous to the principles underlying the vapor pressure formula. The concept of the independence of the average density $\bar{D}$ from the type and the degree of orientation, (1) and (2), is a *conservation principle*, i.e. the number of the grains or vectors is assumed to be constant. The ideal gas equation and a power of cosine are the simplest functions compatible with the respective problems. Finally, we have postulated that an axially symmetric fabric be quantitatively characterized by one single parameter t. This may be an approximation of the same kind as when we regard the heat of evaporation H independent of temperature. It is well known that more complicated vapor pressure formulae result when account is taken of the temperature dependence of H. More complicated formulae, with an increasing number of parameters, have to be used when more precise data are to be evaluated for larger intervals of temperature.

When we extend this, as a loose analogy, to our orientation problem cases may occur where it is no longer possible to describe experimental data by means of the simple formula (9), i.e. with one orientation parameter t. It is easy to verify that (2) is satisfied also by a sum of cosine powers:

$$\begin{aligned} D(\varphi; p_1; p_2 \dots p_n; t_1; t_2 \dots t_n) = \\ = \bar{D}\left(p_1 t_1(\cos\varphi)^{t_1-1} + p_2 t_2(\cos\varphi)^{t_2-1} + \cdots + p_n t_n(\cos\varphi)^{t_n-1}\right) \end{aligned} \tag{11}$$

in which the orientation is characterized by a set of parameters p_n and t_n. These latter have to satisfy two relations:

$$t = \frac{D(0)}{\bar{D}} = p_1 t_1 + p_2 t_2 + \cdots + p_n t_n \tag{12}$$

and, in order to comply with (2):

$$1 = p_1 + p_2 + \cdots + p_n \tag{13}$$

i.e. $2(n-1)$ parameters are independent. Relation (13) suggests that a fabric may be viewed as being composed of discrete portions or domains of minerals, each one of which is characterized by a degree of orientation t_n. Such a view is supported by observations of Tressler and Williamson (1966) and of Smart (1967) on deformed clays. p_n is then the proportion of an entity, denoted by t_n, in the whole fabric.

This more generalized way of describing preferred orientation offers possibilities of a more refined evaluation of experimental data. The two more perfectly oriented kaolin samples K 6_2 and K 16_4, for which the description by the simple function (9) was not entirely perfect at higher φ-angles, may serve as examples. A function composed of two cosine powers:

$$J(\varphi) = \bar{J}\left(p_1 t_1(\cos\varphi)^{t_1-1} + p_2 t_2(\cos\varphi)^{t_2-1}\right) \tag{14}$$

may be determined in such a way that the most reliable $\bar{J}$, that of K I whose description by (9) is the most perfect, is used as a basis. The parameters t_1 and t_2 are taken from the slopes in the logarithmic plot at low and higher φ-angles. The latter region will yield t_2 with rather low accuracy. p_1, and thereby p_2, are then more or less fixed. Fig. 6 shows that the experimental data of K 16_4 yield an almost

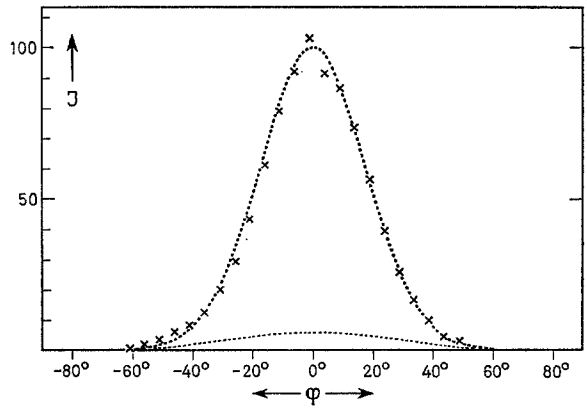

Fig. 6. Description of preferred orientation for K 16_4 by means of two-term function according to (14):

$$J(\varphi) = 9.16 \cdot (0.87 \cdot 11.8 (\cos \varphi)^{10.8} + 0.13 \cdot 5 \cdot (\cos \varphi)^4).$$

The lower curve shows the contribution of the second term. A function of type (19) would yield no better fit than the one-term description (9) in Fig. 4. Therefore, in order to obtain the same degree of concordance as in this figure, an expression composed of two terms of type (19) must be considered

complete fit with a function of two terms. The remaining deviations are due to incomplete axial symmetry. K 6_2 would be more perfectly described by the function (no illustration):

$$J(\varphi) = 9.16 \left(0.95 \cdot 21.0 \cdot (\cos \varphi)^{20.0} + 0{,}05 \cdot 12 \cdot (\cos \varphi)^{11}\right).$$

The numerical parameters for K 16_4 are given in the subscript of Fig. 6.

It may be conceived that the small portions (13 and 5%) of less perfectly oriented clay are located in the slip bands via which the preferred orientation by compression was brought about (conf. Tressler and Williamson).

Function (9) still has one drawback for low values of t, in that it is zero at 90° for any $t > 1$, with the exception of $t = 1$. This is not realistic in view of the current use of the intensity ratio $(00l)/(0k0)$ as an orientation index at low degrees of orientation (Brindley and Kurtossy, Niskanen), which should be ∞ at the slightest orientation according to (9). Moreover, the derivative $\frac{dJ(\varphi)}{d\varphi}$ of (9c) is discontinuous at 90° for $1 < t < 2$. This is an unlikely situation for a natural distribution function, especially, in view of the prospect that a statistical development via a differential equation might be possible. A two term expression

$$J(\varphi) = \bar{J}\left(p_0 + p_T \cdot T \cdot (\cos \varphi)^{T-1}\right) \tag{15}$$

with

$$p_0 + p_T = 1;$$

and

$$t = \frac{J(0)}{\bar{J}} = p_0 + p_T T$$

would be a solution which is not zero at 90°, and it yields a continuous derivative there for $T \geqq 2$. This way, the oriented specimen is regarded as being composed of an unoriented portion p_0 and of a portion p_T, oriented according to T.

However, for particles with a very strong tendency towards parallel orientation on a flat surface, i.e. for particles susceptible to higher values of t, it is very likely that $D(90°)$ is zero. We see this when we inspect a heap of coins or a stack of unanswered mail on a table, or when we try to have a stack of unbound issues of this journal stand up without support. Only for partially bent and crumpled paper (equivalent to the ground clay minerals of Niskanen) or by using supports (equivalent to the presence of isometric grains in a clay, or to bonding the clay with some cement; Brindley and Kurtossy), is it possible to have a measurable amount of paper surface standing perpendicular, i.e. to have $D(90°)$ different from zero. This latter occurs also after the issues of a journal have been bound to thick volumes which in a mixture act as supports for the unbound ones in the same way as the worm-like aggregates in an untreated specimen of a kaolin.

The development of (9) given in this paper imposes no restrictions on t, except that it is (equal to or) greater than unity. However, as developed, function (9) applies only to the upper half of the reference sphere for any t. In order to make it applicable also to the lower hemisphere we proposed to use the absolute value of the cosine as in (9c). This expression does not represent an analytic function at $\varphi = 90°$, in that it does not possess all higher derivatives there for arbitrary values of t. We have already mentioned above that its derivative is discontinuous for $t < 2$. In an analogous fashion the second derivative is continuous only for $t \geqq 3$ and so on. In general, nature appears to favor analytic functions, but at the moment we have no cogent criteria to decide whether the density function should be analytic at 90°, or not. All the same, it is interesting to discuss the conditions for an analytic density function which is valid for both hemispheres without any break at 90°. This is the case in the simple function (9) when t is an odd integer so that the exponent $(t-1)$ of the cosine is even. Consequently, degrees of orientation intermediate between two odd values of t can be described only by a function with at least two even cosine powers:

$$J(\varphi) = \bar{J} \cdot \left(p \cdot (2n-1) \cdot (\cos\varphi)^{2n-2} + (1-p) \cdot (2n+1) \cdot (\cos\varphi)^{2n}\right) \qquad (16)$$

with

$$t = \frac{J(0)}{\bar{J}} = 2n - 2p + 1 .$$

This means that the degree of orientation can no longer be described by one continuously variable parameter. Instead, two parameters, p and n, are necessary. Whereas p is continuously variable between 0 and 1; n has to be an integer and is thus variable only in a discontinuous manner. This way, in order to avoid any discontinuity of the density function at 90°, we have traded a discontinuous variability of t. A decision from experimental data whether such an analytic description of the density is superior to a single cosine power, whose exponent may be odd or fractional, should be most sensitive at low degrees of orientation. For M I, the values of the analytic function:

$$J(\varphi) = 13.2 \cdot (0.375 \cdot 3 \cdot \cos^2\varphi + 0.625 \cdot 5 \cdot \cos^4\varphi) \quad \text{(conf. (16))}$$

are slightly but distinctly different from those of

$$J(\varphi) = 4.25 \cdot 13.2 \cdot (\cos \varphi)^{3.25} \quad \text{(conf. Fig. 3)}$$

except at $\varphi = 0°$ and $\varphi \sim 50°$. The differences are, however, not important enough to allow a definite choice on the basis of the experimental data. These are equally well described both ways. In view of this state of affairs we may as well continue using the more versatile one-term expression for practical purposes, even if the matter should be settled in favor of (16) by a statistical derivation of the density function.

The discussion of the functions with several cosine powers might have suggested that (9) is the only function available as long as we insist on a description of preferred orientation by one single, continuously variable parameter t. Regardless of this impression, functions of the type (11) with several cosine powers will lead us to more expressions characterized by one orientation parameter. In (11), we may employ an infinite number of integer cosine powers and dispose of the p_n in such a way that the sum of the $p_n t_n (\cos \varphi)^{t_n - 1}$ forms a convergent series S. This latter may be regarded as a power series of the variable $(k \cdot \cos \varphi)$, and it may be scaled in such a way that it complies with $t = \frac{D(0)}{\bar{D}}$:

$$D(\varphi, t) = t \cdot \bar{D} \cdot \frac{S(k \cdot \cos \varphi)}{S(k)}. \tag{17}$$

A transcendental relation between t and k can in general be found by taking account of (2). This will certainly be more complicated than the simple arithmetic relation between the two orientation parameters t and $(t-1)$ of (9), if we choose, for a short moment and for sake of analogy, to look upon (9) as being formally determined by two different coefficients as well.

The function $\exp(k \cdot \cos \varphi)$ has been suggested without proof by Fisher (1953) for spherical distributions, and its application to quantitative petrofabric studies has been discussed by Braitsch (1956). It may be regarded as a special case of (17), since the exponential function $\exp(k \cdot \cos \varphi)$ may be expressed as an infinite series of cosine powers. The properly scaled function must be written:

$$D(\varphi, t) = t \cdot \bar{D} \cdot \frac{\exp(k \cdot \cos \varphi)}{\exp(k)} = t \cdot \bar{D} \cdot \exp\big(k \cdot (\cos \varphi - 1)\big). \tag{18}$$

The coefficients are related by: $t = \frac{k}{1 - \exp(-k)}$.

If we want to apply this function also to the lower hemisphere we have to use the absolute value sign on the cosine as in (9c). This way (18) is not differentiable at 90° for any t. These difficulties do not occur when we use a function which is described by an infinite power series with even order terms only. The hyperbolic cosine may serve as an example:

$$D(\varphi, t) = t \cdot \bar{D} \cdot \frac{\cosh(k \cdot \cos \varphi)}{\cosh(k)} \tag{19}$$

and

$$t = k \cdot \coth(k).$$

When compared to the experimental data of K I

$$D(\varphi, t) = 5.1 \cdot 9.16 \cdot \frac{\cosh(5.1 \cdot \cos\varphi)}{\cosh(5.1)}$$

offers no better description than does

$$D(\varphi, t) = 5.1 \cdot 9.16 \cdot (\cos\varphi)^{4.1}$$

in Fig. 4.

Thus there is no practical reason to use (19) or even (18) instead of (9) for the evaluation of experimental data as carried out above. Nontheless, being an analytic function without any discontinuities at 90°, (19) may show advantages in applications where both hemispheres have to be considered.

For larger values of t, and especially at low φ-angles, there will be no appreciable difference between (18) and (19), according to the definition of the hyperbolic cosine as the sum of two exponential functions of the same arguments but of opposite signs, the magnitude of the power with negative exponent becoming negligible.

A closer comparison of (18) and (9) is afforded when we write the latter:

$$D(\varphi, t) = t \cdot \bar{D} \cdot \exp\left((t-1) \cdot \ln\cos\varphi\right). \tag{9f}$$

We have the logarithm of the cosine in the exponent, instead of the cosine itself in (18). In order to study the behavior of (18) and (9f) at lower φ-angles we write the power series for cos φ and ln cos φ consider the first terms only:

$$\cos\varphi = 1 - \frac{\varphi^2}{2} + \cdots : \quad D(\varphi, t) = D(0) \cdot \exp\left(-\frac{k \cdot \varphi^2}{2}\right), \tag{18a}$$

$$\ln\cos\varphi = -\frac{\varphi^2}{2} - \cdots : \quad D(\varphi, t) = D(0) \cdot \exp\left(-(t-1) \cdot \frac{\varphi^2}{2}\right). \tag{9g}$$

We see that for low φ-angles (18) and (9) grade into the same type of function, the Gauss distribution. They can no longer be distinguished at very high degrees of orientation when k, t and $(t-1)$ are practically equal. The most interesting point is that it becomes thus evident under what conditions preferred orientation is described by a Gauss curve or normal distribution. This has been chosen by Dunn (1954) to depict the X-ray intensities of cold rolled metal specimens. The author plotted the logarithm of the diffracted intensity versus the square of the φ-angle and obtained roughly straight lines. This approximate behavior, however, would be expected also for a cosine power function, in view of the prevailing contribution of the square term to the ln cos and cosine series. Because there is no way of having the Gauss distribution comply with (2) and (3), except for extremely high values of t, it cannot be accepted as a generally valid description of preferred orientation.

We may even go one step farther and consider the distribution of errors for the measurement of angles. In the Gaussian description, errors of all magnitudes may occur, albeit with drastically decreasing probability for increasing magnitude. In the measurement of angles, however, errors greater than 90° are hardly imaginable, even with the crudest measuring device imaginable. Moreover, an

error of $90°+\beta$ may be interpreted as $90°-\beta$ when we measure the angle between non-polar directions. Under these circumstances, errors greater than 90° are meaningless, and from this point of view it appears that properly normalized functions of the type

$$F(\alpha) = a(\cos\alpha)^b \quad \text{or perhaps} \qquad F(\alpha) = a \cdot \frac{\cosh(b \cdot \cos\alpha)}{\cosh(b)}$$

may be the adequate distributions of the errors for measured angles. The Gauss distribution is then a mere approximation for the low mean deviations, i.e. for the high accuracy, with which angles are normally measured.

The preceding consideration may suggest that function (9) [or possibly (19)] is perhaps of more general importance. But for the moment its significance lies in the versatility which it affords in the quantitative evaluation of experimental orientation data. When written for the density of a given crystallographic vector, clustered around the pole, it may be used to calculate the density of an other vector which is at an angle with the first. The problem is simple for an angle of 90°. This way, the relation between the density of (*00l*) at the pole and that of (*0k0*) on the girdle around the equator has been determined for oriented aggregates of flake-like clay minerals (Lippmann, 1968). Calculations for angles other than 90° are being attempted.

Zusammenfassung

Texturpräparate blättchenförmiger Tonminerale, wie sie zur Verstärkung der Basisreflexe bei der röntgenographischen Bestimmung hergestellt werden, sind rotationssymmetrische Gefüge. Die Symmetrieachse oder Pol steht senkrecht auf der Oberfläche und fällt mit dem Dichtemaximum der Basislote zusammen. Betrachtet man eine feste Anzahl Blättchen, so kann man fordern, daß die Güte der Orientierung nur von einem einzigen Parameter t abhängt, der als Verhältnis der variablen maximalen zur konstanten durchschnittlichen Lotdichte $\bar{D}$ definiert wird. Der Dichteabfall vom Pol zum Äquator kann dann durch eine Potenz des Cosinus der Polardistanz φ beschrieben werden:

$$D(\varphi, t) = t \cdot \bar{D} \cdot (\cos\varphi)^{t-1}. \tag{9}$$

Diese Formel und ihre Varianten (9a—g) ermöglichen die quantitative Auswertung gemessener Röntgen- und U-Tisch-Gefügedaten.

Die Übereinstimmung zwischen gemessener und berechneter Lotdichte kann in einigen Fällen durch Verwendung einer Summe aus zwei Cosinuspotenzen verbessert werden. Die Cosinuspotenz ist keineswegs die einzige Lösung des Problems. Andere mögliche Lösungen sind jedoch zunächst weniger handlich und liefern keine bessere Beschreibung der Meßwerte. Die Gauß-Verteilung ist eine spezielle Näherung für (9) bei sehr großer Orientierungsgüte.

Acknowledgement. The present study has been stimulated by research of Prof. Dr. W. v. Engelhardt and his co-workers. The experimental data kindly made available for analysis are gratefully acknowledged.

References

Braitsch, O.: Quantitative Auswertung einfacher Gefügediagramme. Heidelberger Beitr. Mineral. Petrog. **5**, 210—226 (1956).

Brindley, G. W., and S. S. Kurtossy: Quantitative determination of kaolinite by X-ray diffraction. Am. Mineralogist **46**, 1205—1215 (1961).

Dunn, C. G.: The analysis of quantitative pole-figure data. J. Appl. Phys. **25**, 233—236 (1954).

Engelhardt, W. v., and K. H. Gaida: Concentration changes of pore solutions during the compaction of clay sediments. J. Sediment. Petrol. **33**, 919—930 (1963).

Fisher, R. A.: Dispersion on a sphere. Proc. Roy. Soc. (London), Ser. A **217**, 295—305 (1953).

Green II, H. W.: Quartz: extreme preferred orientation produced by annealing. Science **157**, 1444—1447 (1967).

Jasmund, K.: Texturaufnahmen von blättchenförmigen Mineralen submikroskopischer Größenordnung in einer Debye-Scherrer-Kamera. Neues Jahrb. Mineral., Monatsh. **3**, 63—72 (1950).

Jetter, L. K., C. J. McHargue, and R. O. Williams: Method of representing preferred orientation. J. Appl. Phys. **27**, 368—374 (1956).

Klug, H. P., and L. E. Alexander: X-ray diffraction procedures, p. 376—378. New York: Wiley 1954.

Lippmann, F.: Enhancement of *(0k0)* reflections of clay minerals in a Guinier camera. Contr. Mineral. and Petrol. **19**, 260—270 (1968).

Niskanen, E.: Reduction of orientation effects in the quantitative X-ray diffraction analysis of kaolin minerals. Am. Mineralogist **49**, 705—714 (1964).

Sander, B.: Einführung in die Gefügekunde geologischer Körper, Bd. II, S. 356—383. Wien: Springer 1950.

Schulz, L. G.: A direct method of determining preferred orientation of a flat reflection sample using a Geiger counter X-ray spectrometer. J. Appl. Phys. **20**, 1030—1033 (1949).

Smart, P.: Particle arrangement in kaolin. Clays and Clay Minerals, Proc. 15th National Conf. **15**, 241—254 (1967).

Taylor, R. M., and K. Norrish: The measurement of orientation distribution and its application to quantitative X-ray diffraction analysis. Clay Minerals **6**, 127—142 (1966).

Thiem, H. J.: Quantitative Texturanalyse durch Röntgenintensitätsmessungen und ihre Anwendung auf experimentell verdichtete Kaolinit- und Montmorillonit-Tone. Diss., Tübingen 1967.

Tressler, R. E., and W. O. Williamson: Particle arrangement and differential imbibition swelling in deformed or deposited kaolinite-illite clay. Clays and Clay Minerals, Proc. 13th National Conf. **13**, 399—410 (1966).

Dr. Friedrich Lippmann
Mineralogisch-Petrographisches Institut der Universität
7400 Tübingen, Wilhelmstr. 56